Comparative micro-Raman spectroscopy study of tellurium-filled double-walled carbon nanotubes

Mariana Sendova, Emmanuel Flahaut

Comparative micro-Raman spectroscopy study of tellurium-filled double-walled carbon nanotubes

Mariana Sendova[1,a)] and Emmanuel Flahaut[2]
[1]*New College of Florida, Sarasota, Florida 34243, USA*
[2]*Centre Interuniversitaire de Recherche et d'Ingenierie des Materiaux (UMR CNRS 5085), Université Paul Sabatier, 31602 Toulouse Cedex 4, France*

Tellurium-filled double-walled carbon nanotubes (Te@DWNTs) have been studied by Raman spectroscopy in the temperature interval from 300 to 700 K employing 785 nm excitation wavelength, and their spectra have been compared to those of pristine double-walled carbon nanotubes (DWNTs). The DWNTs were synthesized by catalytic chemical vapor deposition. Assignment of the radial breathing modes and the tangential modes was done based on the one dimensional electronic energy band structure of carbon nanotubes. The tangential mode components of Te@DWNT are downshifted compared to those of pristine DWNT consistent with the proposed weakening of the carbon-carbon bond due to the introduced van der Waals interaction of the Te atoms with the DWNT. It was established that Te@DWNT can be unambiguously identified by the 30% temperature coefficient decrease of the G′-band position.
DOI: 10.1063/1.2832757

INTRODUCTION

The preparation and investigation of highly anisotropic one dimensional (1D) structures are some of the key objectives in nanoscience. The electronic, optical, thermal, magnetic, and catalytic properties of high aspect ratio nanocrystals are extensively studied. One recent advancement in carbon nanotube research is the production of DWNT filled with a variety of materials along the nanotube axis.[1,2] Double-walled carbon nanotubes (DWNTs) are of special interest because their morphology and properties remain very close to those of single-walled carbon nanotubes, with the main advantage that the outer tube protects the inner one. The introduction of materials into the hollow nanotube cavities could result in interesting effects on their physical and electronic properties thanks to the 1D-like organization of the matter. Here we report results obtained by micro-Raman spectroscopy of Te@DWNT. By comparing the main Raman bands and their temperature coefficients of pristine and filled carbon nanotubes, we find evidence of a decreased interaction between the carbon atoms in the nanotubes as a result of the additional van der Waals interaction between the Te atoms and the carbon nanotube inner wall.

EXPERIMENTAL

DWNTs were synthesized by catalytic chemical vapor deposition as described in a previous paper.[1] They were filled using a high filling yield capillary wetting technique.[2] DWNTs were mixed and gently ground together with Te powder (99.999% purity, Strem Chemicals). The mixture was vacuum sealed in a quartz ampoule which was heated in a programmed furnace at 5 K min^{-1} to 843 K (i.e., above the melting point of Te) followed by a dwell at this temperature for 10 h, followed by cooling first to 743 K at 1 K min^{-1}, then to 673 K at 0.1 K min^{-1}, and then down to room temperature at 1 K min^{-1}. Because of the impossibility to dissolve Te due to its very low solubility in acids, excess of Te located around the DWNT could not be removed by washing, as this is usually the case with soluble compounds.[2,3] Filling yield was roughly estimated to be ~50%, straight from transmission electron microscopy (TEM) observation, Fig. 1.

Raman spectra were acquired using a Leica DMLP microscope coupled to a Raman system manufactured by Kaiser Optical Systems, Inc. The RamanRxn1™ analyzer incorporates the TE-cooled charge coupled device (CCD) detector for maximum sensitivity, Invictus™ NIR semiconductor laser with a wavelength of 785 nm (1.58 eV), and holographic grating to provide fast, simultaneous full spectral collection of Raman data. The spectral resolution of this Raman system is about 5 cm^{-1}. The laser spot diameter on the sample was 10 μm. The size of the laser spot was calibrated using uniform size 1 μm diameter polymer microspheres. The size of the laser spot on the DWNT sample was optimized by maximizing the Raman signal from the same area. The power density was maintained at the lowest level possible at this setup of 15 $\mu W/\mu m^2$. Heating effects from the laser irradiation are negligible at this power density level.[4] The samples

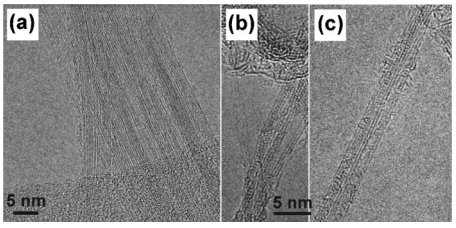

FIG. 1. TEM images of Te@DWNT at different magnifications. Te atoms appear as black dots inside the cavity of the DWNT.

a)Electronic mail: sendova@ncf.edu.

were heated in a Linkam THMS 600 heating stage in static air from 20 to 500 °C at 5 °C/min. Spectra were collected at room temperature and from 50 to 500 °C every 50 °C, after allowing 10 min for thermalization at each temperature point.

All spectra were normalized and fitted using GRAMS/AL 7.02 (Thermo Electron Corporation) and ORIGINPRO (Origin Lab Corporation) softwares. The samples were in a powder form and the DWNTs have a range of diameters, therefore a single spectrum cannot be representative. Statistical average and standard deviation for every band and spectral component discussed in this article were obtained after analyzing 30 (50) spectra collected from different areas for the pristine DWNT sample (Te@DWNT sample) at room temperature. For the temperature studies extreme care was taken to assure identical position of the laser spot at each temperature point.

RESULTS AND DISCUSSION

The radial breading mode (RBM) band is the lowest frequency Raman spectral feature of carbon nanotubes and it is a result of coherent out-of-plane C–C bond stretching in radial direction.[5] The position of the Lorentzian components of the RBM band is directly related to the nanotube diameter. Given the significant diameter distribution of DWNT in the powder sample,[1] even when micron sized spot of the excitation radiation is used, the RBM band becomes a superposition of considerable number of Lorenzians. Since neither the number of the spectral components nor their linewidth can be determined before hand, only rough diameter estimates can be carried out using the most prominent RBM spectral features. In addition, instrument resolution limitations do not allow us to detect any splitting of the carbon nanotubes Raman lines, due to the Te atoms inside the CNTs as predicted theoretically by Bose *et al.*[6] The RBM band of Te@DWNT is shown in Fig. 2(a). While the electronic structure depends on tube diameter, Raman scattering resonance follows the electronic structure of the tube. According to the calculations for the energy separation between mirror-image electronic density of states van Hove singularities, E_{ii} as a function of the nanotube diameter, the energy of the excitation photons in our experiment (1.58 eV) matches the E_{11}^{M} for larger diameter, 1.59 nm (most probably outer) metallic nanotubes, and the E_{22}^{S} for smaller diameter, 1.05 nm (most probably inner) semiconducting nanotubes.[7] It is common, at the given photon excitation, to detect a range of diameters at 1.5–1.7 nm for metallic carbon nanotubes (CNTs) and 1.0–1.1 nm for semiconducting CNTs to be detected which electronic transitions fall into ±0.1 eV from the incident photon excitation energy.[8] The position of the RBM components is estimated by multi-Lorentzian least square fitting performed in the range of 120–290 cm^{-1}, Fig. 2(a). The position, width, and the intensity of each Lorentzian line shape were free fitting parameters. Typically, the minimum number of spectral components allowing satisfactory RBM band fit was 8. Their full width at half maximum (FWHM) varied between 10 and 30 cm^{-1}. There was not any detectable systematic difference in the components of the RBM band between the pristine and filled DWNT samples. The corresponding RBM spectra of the pristine and Te@DWNT are overlaid in Fig. 2(b). The positions of the resolved components of the RBM bands are summarized in column 2 of Table I. As first approximation, DWNT diameter estimate can be done by applying the empirical relation: $d_{exp}=248/\omega$, which was established by resonant Raman scattering of individual single-walled carbon nanotubes (SWNTs).[8] The SWNT relation has been implemented for estimating the diameters of the two carbon shells constituting a single DWNT.[9,10] In order to characterize the

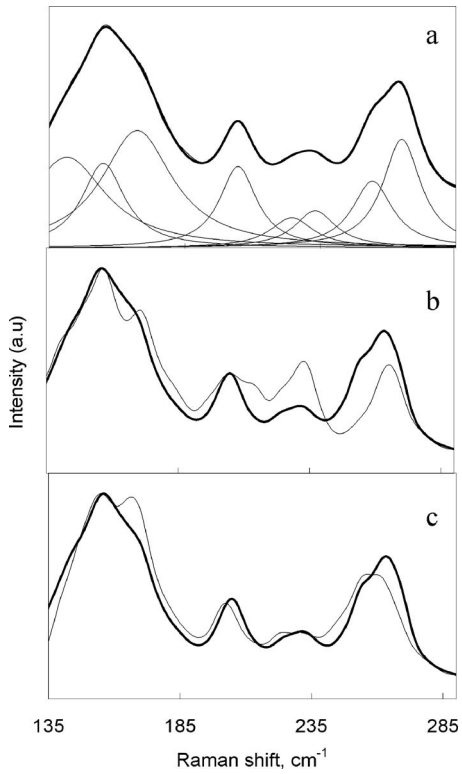

FIG. 2. (a) RBM band of Te@DWNT at room temperature fitted with a sum of Lorentzians. (b) RBM bands of pristine and Te@DWNT (bold trace) at 296 K. (c) RBM bands of Te@DWNT at 296 K (bold trace) and at 673 K.

TABLE I. RBM frequencies of Te@DWNT, estimated diameters, assigned indices, and corresponding electronic transitions. RBM frequencies of SWNT in resonance with 1.58 eV laser excitation calculated according to Kataura *et al.* (Ref. 7) are presented for comparison in column 1.

SWNT	DWNT			
	$\omega \pm 1$ (cm^{-1})	d_{exp} (nm)	(n,m)	E_{ii} (eV)
	139–144	1.79–1.72	?	?
147, 148, 149, 153				
155, 156	**156**	**1.59**	**(13, 10)**	**1.58**
159, 160, 162				
167	**167**	**1.49**	**(15, 6)**	**1.68**
	170	1.46	(16, 4)	1.72
	200–210	1.24–1.2	(9, 9)	2.02
220, 221, 223				
225	**225**	**1.1**	**(9, 7)**	**1.51**
232	**233**	**1.07**	**(11, 4)**	**1.56**
236, 238, 240, 245, 249				
	254	0.98	(9, 5)	1.71
	263	0.94	(8, 6)	1.73

electronic properties of the CNTs, and thus assign the spectral features of the Raman G band, the chiral vector components (n,m) are determined, based on their relation to the CNT diameter $d=/a_{c-c}\sqrt{3(m^2+mn+n^2)}/\pi$, column 4 of Table I. The resonant energy associated with the experimentally determined CNT diameter is calculated based on the tight binding model (the transfer integral is $\gamma_o=2.9$ eV, and the C–C distance is $a_{C-C}=0.144$ nm)[8] and presented in the last column of the same table. For the semiconducting nanotube (most probably inner) resonant energy difference occurs at $E_{22}^S(d)=2E_{11}^S=4a_{c-c}\gamma_o/d$ and for the metallic (most probably outer) nanotube resonant energy occurs at $E_{11}^M(d)=6a_{c-c}\gamma_o/d$.[11] The transition energies are summarized in column 5 of Table I. The RBM modes for SWNT at 785 nm laser excitation line are listed in the first column of the same table for comparison reasons. Four components of the RBM band can be assigned following SWNT approximation. One of them is the most intense low frequency component (156 cm^{-1}), attributed to a metallic (13,10) nanotube shell. The SWNT model for the CNT with a diameter of 0.94 nm yields an energy of 1.73 eV, which is outside of the accepted resonant window. The smallest SWNT diameter having transition energy within the resonant window 1.58 ± 0.1 eV is 1.05 nm. However, according to the same SWNT model, for 1.05 nm diameter nanotube the RBM mode should be at 249 cm^{-1}, which is 14 cm^{-1} lower than the detected component. Given the fact that the detected nanotubes have to be in resonance with the incident radiation, (1.58 eV) we can conclude that there is an energy increase in the corresponding interband optical transition in DWNT in comparison to the SWNT. This increase results in an upshift of the RBM mode of the CNT as compared to the corresponding RBM mode of a SWNT with the same diameter (1.05 nm). Similar reasoning can be applied for the assignment of the 170, 200-210, and 254 cm^{-1} components. Theoretical justification for the RBM mode upshift is found in calculations performed for breathinglike phonon modes in double-walled[12,13] and multiwalled[14] carbon nanotubes. The calculations indicate frequency upshift in comparison to the RBM position of a single nanotube with a given diameter due to carbon shell interaction. Low temperature high resolution Raman studies confirmed the frequency upshift of the RBM modes for both inner and outer CNTs up to 12 cm^{-1}.[15] High resolution Raman measurements may reveal the existence of any splitting of Raman peaks due to the presence of the Te atoms inside the CNT, as theoretically suggested.[6] At the resolution level of our instrument we were able to detect only consistent increase of the FWHM of the two most intense RBM components (156 and 263 cm^{-1}) in the filled DWNT as compared to the pristine DWNT. Our studies indicate weak temperature dependence of the RBM components both for pristine and filled DWNT. The RBM bands of Te@DWNT at room temperature and at 400 °C are presented for comparison at Fig. 2(c). As can be seen, at 400 °C the maximum component upshift is 2 cm^{-1}, accounting for a temperature coefficient not larger than 0.5×10^{-2} cm^{-1}/K and there is no apparent dependence on the tube diameter. The temperature coefficient and its independence from the tube diameter is in agreement with the temperature study of the RBM band of individual SWNT on SiO_2 substrate at 632 nm excitation.[16] However, another Raman spectroscopy temperature study[17] of DWNT (synthesized by floating catalyst chemical vapor deposition) at 632 nm laser excitation line indicated RBM temperature coefficient decrease for the high frequency RBM components. The results from our study are in agreement with the temperature coefficient of the highest frequency component of the RBM band reported by Ci *et al.*[17]

G band (TM band in some references) is the most intense Raman spectral feature (1550–1600 cm^{-1}). It is a result of tangential C–C bond stretching. The position and the line shape of the G-band components are different for semiconducting and metallic CNTs.[18] Therefore, the G band in our study requires contribution from both semiconductor and metallic CNT spectral features. It has been established that the G band of the metallic SWNT consists of two components: a Lorentzian line shape higher frequency component at around 1580 cm^{-1} and a Breit-Wigner-Fano (BWF) line shape component at lower frequencies ~1545 cm^{-1}. The asymmetric BWF line shape is described by[19]

$$I(w)=I_o\frac{[1+(\omega-\omega_o)/q\Gamma]^2}{1+[(\omega-\omega_o)/\Gamma]^2},$$

where $1/q$ has a negative value and is a measure of the electron-phonon coupling, ω_o is the peak frequency at maximum intensity I_o. BWF function was used to fit some of the Raman bands of the metallic forms of sp^2 carbons in metallic SWNT[20] and DWNT.[9] For very small $|1/q|$ parameters the function becomes a Lorentzian. The number of components of the G band of semiconducting SWNT predicted by the group theory is six and has been well explained.[20] Symmetry assignments of four Lorentzian components of the G band [~1549 cm^{-1} ($\omega_{E_2}^-$), ~1567 cm^{-1} (ω_G^-), ~1590 cm^{-1} (ω_G^+), and ~1607 cm^{-1} ($\omega_{E_2}^+$)] of single semiconducting SWNT have been reported.[21,22] Following the theoretical predictions one should expect at least six G-band components when semiconducting and metallic CNTs are present. However, in a first approximation, for comparative reasons we analyzed the G band of the DWNT powder samples by fitting it with the minimum number of Lorentzians and one BWF line shape reflecting the assignments suggested from the most prominent features of the RBM band. The G-band profile of all DWNT samples can be fitted satisfactory with two Lorentzian line shapes and one BWF function, see Fig. 3(a). Employing more than three components without knowing their position and width can be ambiguous and subjective. The position (ω) and the FWHM (Γ) of each G-band component for the pristine and filled nanotubes are summarized in Table II. The standard deviation due to the uncertainties of the fitting is estimated as well. The BWF component in our fit can be considered a superposition of the metallic BWF component and the ω_G^- component of the semiconducting nanotubes. The strong graphitelike feature can be associated to ω_G^+ mode, and the higher frequency Lorentzian line shape to the $\omega_{E_2}^+$ component of a semiconducting shell. This assignment of the Lorentzian G-band components is in a good agreement with the assignment of the G band of empty DWNT powder samples reported by Puech and

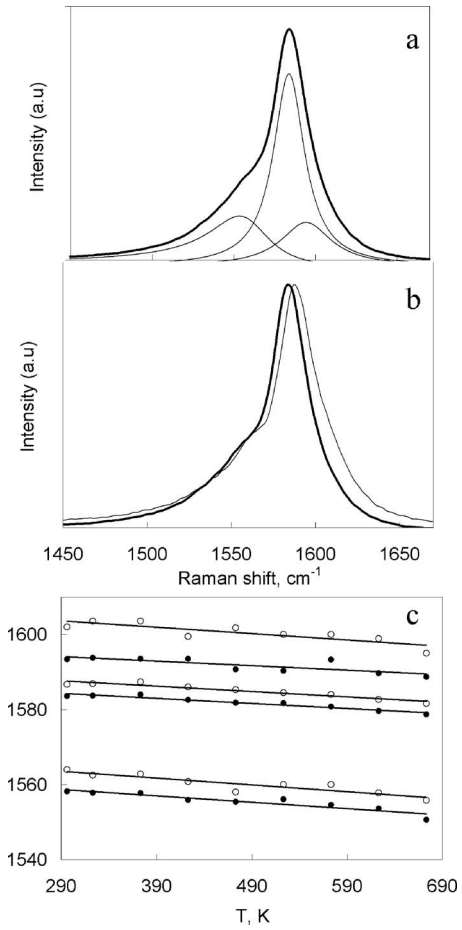

FIG. 3. (a) G band of Te@DWNT at 296 K fitted by BWF and two Lorentzian line shapes. (b) G bands of pristine and Te@DWNT (bold trace) at 296 K. (c) Temperature dependence of each component of the G band of pristine DWNT (empty symbols) and Te@DWNT (filled symbols).

co-workers[23,24] at 514, 568, and 647 nm Raman excitation wavelengths. The BWF component of filled DWNT is broader, downshifted, and has a smaller interaction parameter $1/q$ in comparison to those parameters in pristine DWNT samples. The other two components of the G band exhibit a downshift too. Moreover, the higher frequency Lorentzian associated with the inner semiconducting nanotubes has the largest downshift of 9 cm^{-1}. The G bands of pristine and Te@DWNT at room temperature are compared in Fig. 3(b). Similarly, other authors report that the G band of SWNT exhibit a downshift associated with increased curvature effects in smaller diameter metallic tubules.[20] On the other hand, curvature effects are associated with admixture of sp^3 character into the sp^2-sp^2 C–C interaction. Since, the C–C sp^3 bond is weaker than C–C sp^2 bond, downshift in the G-band component in smaller diameter SWNT is associated with weakening the C–C bond and thus downshift of the Raman line. Therefore, the experimentally established trend in the position of each of the G-band components of the Te@DWNT might indicate weakening of the C–C bond as a result of the additional van der Waals interaction of the filling Te atoms. In addition, support of these considerations can be found in the published findings of the G-band (1580 cm^{-1}) downshift, up to 5 cm^{-1}, proportionally to the number of graphene layers, attributed to the additional van der Waals interactions between the layers.[25]

The temperature dependence of each one of the G-band components for both samples is presented in Fig. 3(c). The temperature coefficients and the corresponding intercepts are summarized in columns 6, 7, 12, and 13 in Table II. For comparison, the measured value of the temperature coefficient of the G mode (1582 cm^{-1}) of highly oriented pyrolitic graphite (HOPG) is 0.011 cm^{-1}/K.[26] The temperature coefficient of the Lorentzian component ($\omega^{+}_{E_2}$) associated with the Te filled semiconducting nanotubes has a value closest to that of HOPG and it is about 30% smaller compared to that of the pristine DWNT. The change of phonon frequency with temperature stems from the anharmonic terms in the lattice potential energy. In general, two main effects contribute to the phonon shift: purely thermal effect $(\partial\omega/\partial T)_V$ and volume related effect due to lattice expansion $(\partial\omega/\partial V)_T(\partial V/\partial T)_P$. The thermal expansion coefficient of the tube diameter and the lattice constant for SWNT are very small and are experimentally determined by x-ray diffraction studies to be of the order of 0.15×10^{-5} and 0.75×10^{-5} K^{-1}, respectively, between 300 and 950 K.[27] Therefore, the pure thermal effect, but not the volume expansion effect, determined the temperature coefficients of the components in the G band.[5,17] The intrinsic physical origin of the pure thermal effect of the Raman spectrum temperature shift is the temperature dependence of the C–C force constant which is proportional to the square of the phonon frequency.[28] Our experimental results for the G-band temperature coefficients suggest that weakening the C–C force constant leads to a decrease in the corresponding temperature coefficient. This is in agreement with our previous experimental results for PbI_2@DWNT heated by laser irradiation.[29] The proportionality between temperature coefficient and bond strength in SWNT is manifested in the relative magnitudes of the temperature coefficients of the RBM, D band, and G band, increasing in this order.[30,31] The position of the G band, it temperature coefficient, and the variation of these values across the powder sample obtained from this study are summarized in the second row of Table III.

TABLE II. G-band components, position, width, relative intensity, temperature coefficient, and intercept for pristine DWNT and Te@DWNT.

	DWNT						Te@DWNT					
G-band components	ω (cm^{-1})	Γ ($cm^{-1}\pm2$)	$1/q$	Relative intensity	$d\omega/dT$ (10^{-2} cm^{-1}/K)	Intercept (cm^{-1})	ω (cm^{-1})	Γ ($cm^{-1}\pm2$)	$1/q$	Relative intensity	$d\omega/dT$ (10^{-2} cm^{-1}/K)	Intercept (cm^{-1})
BWF	1564 ± 2	38	0.3 ± 0.1	0.25	-1.8 ± 0.2	1569	1558 ± 2	42	0.2 ± 0.1	0.25	-1.7 ± 0.2	1564
Lorentzian 1	1587 ± 0.5	22		1	-1.4 ± 0.1	1592	1584 ± 0.5	21		1	-1.4 ± 0.1	1588
Lorentzian 2	1602 ± 2	42		0.4	-1.7 ± 0.2	1609	1593 ± 2	40		0.3	-1.2 ± 0.2	1598

TABLE III. D, G, and G′-band positions, width, relative intensity, temperature coefficient, and intercept for pristine and Te@DWNT.

	Pristine DWNT					Te@DWNT				
	ω (cm^{-1})	Γ (cm^{-1})	Relative intensity	$d\omega/dT$ (10^{-2} cm^{-1}/K ± 0.1)	Intercept (cm^{-1})	ω (cm^{-1})	Γ (cm^{-1})	Relative intensity	$d\omega/dT$ (10^{-2} cm^{-1}/K ± 0.1)	Intercept (cm^{-1})
D band	1299 ± 2	64 ± 3	0.18 ± 0.08	-1.5	1306	1297 ± 3	78 ± 4	0.15 ± 0.03	-1.2	1302
G band	1587 ± 2	34 ± 2	1	-1.5	1593	1584 ± 2	30 ± 1	1	-1.4	1589
G′ band	2571 ± 3	75 ± 5	0.43 ± 0.04	-2.6	2579	2578 ± 3	76 ± 2	0.38 ± 0.03	-1.8	2584

The D and G′ bands (2D band in some references) are due to one- and two-phonon second order Raman scattering processes, respectively.[32] D band in the Raman spectra of the carbon nanotubes is a result of scattering in the presence of in-plane defects lowering the symmetry of the crystalline lattice. Its overtone, the G′ band is an intrinsic property of any sp^2 carbon material. Therefore, it is not selective to the CNT diameter (as RBM and G bands) and it is much more intense than the disorder-induced D band, and is observed even when the D band is absent (in crystalline graphite).[5] The relative intensities of the D and G′ bands in our samples and their variation across the sample are summarized in Table III. The D and G′ bands were fitted satisfactory by a single Lorentzian component, Figs. 4(a) and 4(c). The position, FWHM, and the relative intensity of both bands across the sample of pristine and filled DWNT are summarized in Table III. Overall, the G′ band is less intensive in the Te@DWNT samples. On average, the G′ band of Te@DWNT is upshifted. This is in agreement with our previous study of PbI_2@DWNT.[29] In addition, Ferrari[25] reports experimentally found upshift of the G′ band of multilayer graphene in comparison to the single layer graphene attributed to additional van der Waals interactions between multiple graphene sheets. The results from the temperature study of the D and G′ bands are presented in Figs. 4(b) and 4(d). The temperature coefficients and the intercepts calculated from the linear fit for each Raman band are included in Table III. The most prominent characteristic distinguishing the Te@DWNT from the pristine DWNT is the significant decrease of their G′-band temperature coefficient, ~30%. The temperature dependence of the G′ band may be a useful practical method for characterization and distinguishing filled from pristine DWNT powders.

CONCLUSIONS

Systematic comparative experimental temperature study (300–700 K) of the most prominent Raman bands of Te@DWNT in powder form was carried out. Frequency downshift of the G-band components is established. 30% decrease of the temperature coefficients of the G-band inner tube component and the G′-band is experimentally determined. Weakening of the sp^2 C–C bond as a result of the additional van der Waals interaction introduced by the filling Te atoms is suggested. The temperature coefficients of the high frequency G-band component and the G′ band are found to be a sensitive probe for distinguishing between filled and unfilled DWNTs.

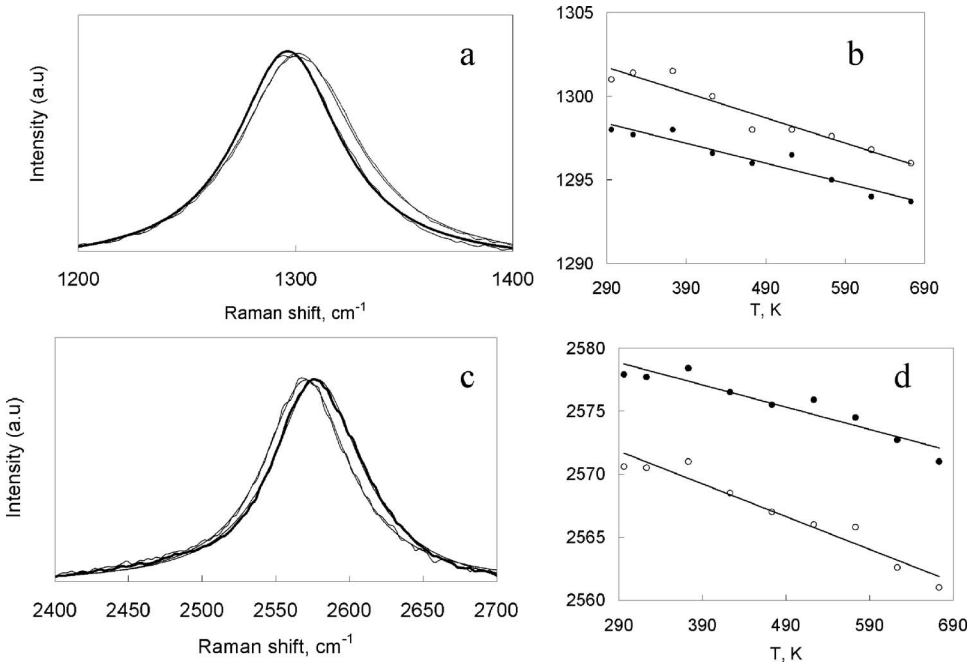

FIG. 4. (a) D band of pristine DWNT and Te@DWNT (bold trace) at 296 K. (b) Temperature dependence of the D band of pristine DWNT (empty symbols) and Te@DWNT (filled symbols). (c) G′ band of pristine DWNT and Te@DWNT (bold trace) at 296 K. (d) Temperature dependence of the G′ band of pristine DWNT (empty symbols) and Te@DWNT (filled symbols).

ACKNOWLEDGMENTS

M.S. thanks Michael Aldridge for helping with some of the data acquisition, and to Dr. Valentin Zhelyaskov for the insightful discussions. Part of the work is done with the financial support of the Faculty Development Fund at New College of Florida. E.F. would like to thank Dr. J. Sloan for help with HRTEM observations.

[1]E. Flahaut, R. Bacsa, A. Peigney, and Ch. Laurent, Chem. Commun. (Cambridge) 1442 (2003).
[2]G. Brown, S. R. Bailey, M. Novotny, R. Carter, E. Flahaut, K. S. Coleman, J. L. Hutchison, M. L. H. Green, and J. Sloan, Appl. Phys. A: Mater. Sci. Process. **76**, 457 (2003).
[3]E. Flahaut, J. Sloan, S. Friedrichs, A. I. Kirkland, K. S. Coleman, V. C. Williams, N. Hanson, J. L. Hutchison, and M. L. H. Green, Chem. Mater. **18**, 2059 (2006).
[4]A. Bassil, P. Puech, L. Tubery, W. Bacsa, and E. Flahaut, Appl. Phys. Lett. **88**, 173113 (2006).
[5]M. S. Dresselhaus and P. C. Eklund, Adv. Phys. **49**, 705 (2000).
[6]S. M. Bose, S. N. Behera, S. N. Sarangi, and P. Entel, Physica B **351**, 129 (2004).
[7]H. Kataura, Y. Kumazawa, Y. Maniwa, I. Umezi, S. Suzuki, Y. Ohtsuka, and Y. Achiba, Synth. Met. **103**, 2555 (1999).
[8]A. Jorio, R. Saito, J. H. Hafner, C. M. Lieber, M. Hunter, T. McClure, G. Dresselhaus, and M. S. Dresselhaus, Phys. Rev. Lett. **86**, 1118 (2001).
[9]S. Bandow, G. Chen, G. U. Sumanasekera, R. Gupta, M. Yudasaka, S. Ijima, and P. C. Eklund, Phys. Rev. B **66**, 075416 (2002).
[10]F. Li, S. G. Chou, W. Ren, J. A. Gardecki, A. K. Swan, M. S. Ünlü, B. B. Goldberg, H.-M. Cheng, and M. S. Dresselhaus, J. Mater. Res. **18**, 1251 (2003).
[11]R. Saito, G. Dresselhaus, and M. S. Dresselhaus, Phys. Rev. B **61**, 2981 (2000).
[12]E. Dobardzic, J. Maultzsch, I. Milosevic, C. Thomsen, and M. Damnjanovic, Phys. Status Solidi B **237**, R7 (2003).
[13]J. Cambedouzou, J.-L. Sauvajol, A. Rahmani, E. Flahaut, A. Peigney, and C. Laurent, Phys. Rev. B **69**, 235422 (2004).
[14]V. N. Popov and L. Henrard, Phys. Rev. B **65**, 235415 (2002).
[15]R. Pfeifer, Ch. Kramberger, F. Simon, H. Kuzmany, V. N. Popov, and H. Kataura, Eur. Phys. J. B **42**, 345 (2004).
[16]Z. Zhou, X. Dou, L. Ci, L. Song, D. Liu, Y. Gao, J. Wang, L. Liu, W. Zhou, and S. Xie, J. Phys. Chem. B **110**, 1206 (2006).
[17]L. Ci, Z. Zhou, L. Song, X. Yan, D. Liu, H. Yuan, Y. Gao, J. Wang, L. Liu, W. Zhou, G. Wang, and S. Xie, Appl. Phys. Lett. **82**, 3098 (2003).
[18]S. D. M. Brown, P. Corio, A. Marucci, M. S. Dresselhaus, M. A. Pimenta, and K. Kneip, Phys. Rev. B **61**, R5137 (2000).
[19]M. V. Klein, in *Light Scattering in Solids I*, edited by M. Cardona (Springer-Verlag, Berlin, 1983), pp. 169–172.
[20]S. D. M. Brown, I. Jorio, P. Corio, M. S. Dresselhaus, G. Dresselhaus, R. Saito, and K. Kneipp, Phys. Rev. B **63**, 155414 (2001).
[21]A. Jorio, A. G. Souza Filho, G. Dresselhaus, M. S. Dresselhaus, A. K. Swan, M. S. Unlü, B. B. Goldberg, M. A. Pimenta, J. H. Hafner, C. M. Lieber, and R. Saito, Phys. Rev. B **65**, 155412 (2002).
[22]A. Jorio, G. Dresselhaus, M. S. Dresselhaus, M. Souza, M. S. S. Dantas, M. A. Pimenta, A. M. Rao, C. Liu, and H. M. Cheng, Phys. Rev. Lett. **85**, 2617 (2000).
[23]P. Puech, E. Flahaut, A. Bassil, T. Juffman, F. Beneu, and W. S. Bacsa, J. Raman Spectrosc. **38**, 714 (2007).
[24]P. Puech, E. Flahaut, A. Sapelkin, H. Hubel, D. J. Dunstan, G. Landa, and W. S. Bacsa, Phys. Rev. B **73**, 233408 (2006).
[25]A. Ferrari, Solid State Commun. **47**, 143 (2007).
[26]P. H. Tan, Y. M. Deng, Q. Zhao, and W. C. Cheng, Appl. Phys. Lett. **74**, 1818 (1999).
[27]Y. Maniwa, R. Fujiwara, H. Kira, H. Tou, H. Kataura, S. Suzuki, Y. Achiba, E. Nishibori, M. Takata, M. Sakata, A. Fujiwara, and H. Suematsu, Phys. Rev. B **64**, 241402 (2001).
[28]R. A. Jishi, L. Venkataraman, and M. S. Dresselhaus, Chem. Phys. Lett. **209**, 77 (1993).
[29]M. Sendova, E. Flahaut, and B. DeBono, J. Appl. Phys. **98**, 4304 (2005).
[30]Ph. Huong, R. Cavagnat, P. Ajayan, and O. Stephan, Phys. Rev. B **51**, 10048 (1995).
[31]F. Huang, K. T. Yue, P. Tan, S.-L. Zhang, Z. Shi, X. Zhou, and Z. Gu, J. Appl. Phys. **54**, 4022 (1998).
[32]M. S. Dresselhaus, G. Dresselhaus, R. Saito, and A. Jorio, Phys. Rep. **409**, 47 (2005).